Pure and Applied Mathematics Quarterly
Volume 8, Number 4
1075—1095, 2012

Computation of Hyperbolic Geometric Flow on Closed Riemann Surfaces

Zheng Xie* and Zheng Ye

Abstract: Hyperbolic geometric flow, introduced by Kong and Liu, is a system of nonlinear evolution partial differential equations of second order for Riemannian metric and Ricci curvature. This work introduces two numerical algorithms for initial value problem of this flow on closed Riemann surfaces with circle packing metric and pointwise conformal metric, and demonstrates the evolution of metric by data and graphs. Specially, the numerical experiment and the analysis of schemes show that the Euler character is an essential obstruction to the existence of periodic solution for any initial metrics on sphere and double torus.

Keywords: Hyperbolic geometric flow, Riemann surfaces, Discrete meric, Circle packing metric, Discrete curvature.

1 Introduction

Let $\mathfrak{M}$ be n-dimensional Riemannian manifold with Riemannian metric g_{ij}. The following general evolution equations for the metric g_{ij} and Ricci curvature R_{ij}

$$\frac{\partial^2 g_{ij}}{\partial t^2} = -2R_{ij} \tag{1}$$

Received August 31, 2010
MSC(2010): 14H55, 37E35, 53C44,52C26.
*This work is partially supported by NUDT Preparing Research Project (JC110204) and National Natural Science Foundation of China (No. 11001237)

have been introduced recently by Kong and Liu motivated by Einstein equation and Ricci flow [1–5] and named hyperbolic geometric flow(HGF), which can be used to describe the wave character of metrics and curvatures of manifolds and carries many interesting features of both the Ricci flow as well as the Einstein equations [6–14]. This is essentially different from the Ricci flow, which describe the heat diffusion process character of metrics and curvatures.

In this paper, we mainly focus on the numerical computation of the initial problem of HGF on closed Riemann surfaces, namely a compact manifold without boundary, such as sphere, torus and double torus. The reason for calculating on closed manifold is because that this surface has a triangulation with a finite number of triangles, and no need to consider boundary conditions, e.g. Dirichlet conditions. As the first part of our research on this topic, we are interested in the computation using Thurston's circle packing on surfaces. This is based on works of the discrete Ricci flow on piecewise linear surfaces introduced by Gu et al [15–18]. As the second part of our research, we are interested in the pointwise conformal class $(\mathfrak{M}, w(t,\cdot)g_0)$, where $w(t,\cdot)$ is a nonnegative function with parameter t and g_0 is the initial metric on the surface. Therefore, the Ricci curvature is

$$R = \frac{2}{w}\left(k - \frac{1}{2}\Delta_{g_0} \ln w\right),$$

where k is the Gaussian curvature of $(\mathfrak{M}, g_0)$. Thus, HGF can be deduced to

$$\frac{\partial^2 w}{\partial t^2} = \Delta_{g_0} \ln w - 2k. \tag{2}$$

We give a numerical algorithm for initial value problem of Eq.(2) on closed Riemann surface, such as sphere and tours. The numerical experiments verify the qualitative conclusions presented by Kong and Liu et al, including the theorem: if the Euler characteristic number of surface is positive, then any solution of Eq.(2) must decay in finite time for any initial problem.

2 Computation of HGF for circle packing metric

Computational domain

A closed Riemann surface has a triangulation with a finite number of triangles, and the Riemannian metric and the Gaussian curvature are discretized as the edge lengths and the angle deficits. In this section, we compute the HGF with circle packing metric. This method is same as discrete Ricci flow, except the different for derivative of time. Consider a triangle mesh Σ for $\mathfrak{M}$ with vertices V, edges E and triangles F. If each triangle in F is realizable on the Euclidean plane, then we call Σ is with Euclidean background geometry. Similarly, the meshes can be defined with spherical or hyperbolic background geometries respectively. Some concepts in differential geometry, such as metric, Gaussian curvature, and conformal structure can also be defined on mesh.

Discrete Riemannian metric

Consider a triangle f_{ijk} with edge lengths l_{ij}, l_{jk}, l_{ki}, and the angles θ_k, θ_i, θ_j against the corresponding edges. The edge lengths define the discrete Riemannian metric on Σ by

$$l : E \to \mathbb{R}^+,$$

such that for a triangle f_{ijk} the edge lengths satisfy the triangle inequality

$$l_{ij} + l_{jk} > l_{ki}.$$

Discrete Gaussian curvature

The discrete Gaussian curvature K_i on a vertex v_i can be computed using Gaussian Bonnet formula from the angle deficit:

$$K_i = 2\pi - \sum_{f_{ijk} \in F} \theta_i^{jk}, \tag{2}$$

where θ_i^{jk} represents the corner angle attached to vertex v_i in the face f_{ijk}. The values of angles and edge lengths are related by cosine laws. Meshes with Eu-

clidean background geometries require the cosine laws as follows:

$$l_{ij}^2 = l_{jk}^2 + l_{ki}^2 - 2l_{jk}l_{ki}\cos\theta_k, \tag{3}$$

where l_{ij}, l_{jk}, l_{ki} are edges in a triangle f_{ijk} and θ_k is the angle attached to vertex v_k.

Discrete conformal structure

Let Γ be a function defined on the vertices

$$\Gamma : V \to \mathbb{R}^+,$$

which assigns a radius r_i to the vertex v_i. Let Φ be a function defined on the edges,

$$\Phi : E \to [0, \frac{\pi}{2}],$$

which assigns an acute angle $\Phi(l_{ij})$ to each edge l_{ij}. The pair (Γ, Φ) on the mesh Σ is called a circle packing metric of Σ. Two circle packing metrics $(\Gamma_1; \Phi_1)$ and $(\Gamma_2; \Phi_2)$ on a same mesh are conformal equivalent, if $\Phi_1 = \Phi_2$.

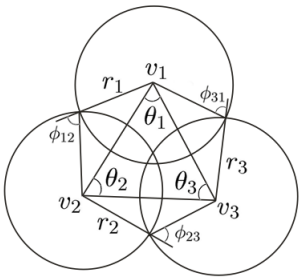

Figure 1: Circle packing metric for a triangle

The circle packing metric and the edge lengths can be converted to each other by using cosine laws dependent on the Euclidean background geometry as follows:

$$l_{ij}^2 = r_i^2 + r_j^2 + 2r_i r_j \cos\phi_{ij} \tag{4}$$

where v_i has a circle whose radius is r_i, ϕ_{ij} is defined by the two circles of v_i and v_j (see Fig.1).

Discrete HGF

Now, we are ready to derive the discrete HGF(DHGF) on surfaces, which is an system of evolution difference equations of the discrete metric. Let

$$u_i = \log r_i. \tag{5}$$

Since the discrete Ricci flow [18] is defined as:

$$\frac{du_i(t)}{dt} = -2K_i,$$

we can similarly derive the DHGF as:

$$\frac{d^2u_i(t)}{dt^2} = -2K_i. \tag{6}$$

The temporal partial derivatives can be approximated by differences. The computational scheme for Eqs.(6) is

$$u_i^{n+1} = -2(\Delta t)^2 K_i^n + 2u_i^n - u_i^{n-1}. \tag{7}$$

where u_i^n denotes $u_i(n\Delta t)$.

Geometric properties

The first geometric property is that the metrics on surfaces at each time step is conformal to the original metrics, since Φ is invariant in the computational progresses. The other geometric property is that the Euler characteristic number has essential relationship with the solution for Eqs.(7). More accurately, we have

Theorem 2.1 *Let $\chi(\mathfrak{M})$ be the Euler characteristic number for closed Riemann surface $\mathfrak{M}$ with triangulation Σ. If $\{u_i^n | i \in V\}$ is a solution of Eqs.(2), then*

a. *If $\chi(\mathfrak{M}) < 0$, then the discrete metric for Eqs.(7) expand in infinite time for any initial value $\{u_i^0, u_i^1 | i \in V\}$.*

b. *If $\chi(\mathfrak{M}) = 0$ and $u_i^1 < u_i^0$ for all $i \in V$, then the discrete metric for Eqs.(7) decay in infinite time;*

c. *If $\chi(\mathfrak{M}) > 0$, then the discrete metric for Eqs.(7) decay in infinite time for any initial value $\{u_i^0, u_i^1 | i \in V\}$.*

Proof. Taking integration on both sides of Eqs.(7) and using Gauss-Bonnet formula, we have

$$\sum_{i\in V} u_i^n = -2n(n-1)\pi\chi(\mathfrak{M})\Delta t^2 + n\sum_{i\in V} u_i^1 - (n-1)\sum_{i\in V} u_i^0 \tag{8}$$

for $n \geqq 2$ and any initial values $\{u_i^1, u_i^0 | i \in V\}$. The conclusions (a-c) can be concluded from (5) and (8). □

It can be see that Euler character is the essential geometric obstruction to the existence of periodic solution on sphere and double torus.

Algorithm

The numerical algorithm to compute Riemannian metrics with prescribed Gaussian curvatures using DHGF is designed. The unified pipeline for this algorithm is listed as follows:

Step 1. **Compute the discrete Gaussian curvature.**

This curvature can be computed from Eq.(2) using Gaussian Bonnet formula.

Step 2. **Compute the initial circle packing metric.**

2.1. For each face f_{ijk}, compute a radius for the vertex v_i

$$r_i^{jk} = \frac{l_{ki} + l_{ij} - l_{jk}}{2},$$

where l_{ij}, l_{jk}, and l_{ki} are the lengths of the edges e_{ij}, e_{jk}, and e_{ki}, respectively.

2.2. For each vertex v_i, approximate the radius r_i by averaging the radius from the faces adjacent to v_i:

$$r_i = \frac{1}{m}\sum_{f_{ijk}\in F} r_i^{jk},$$

where m is the number of the adjacent faces to vertex v_i.

2.3. For each edge l_{ij}, compute its edge weight ϕ_{ij} from r_i, r_j using a cosine law (4). If the edge weight is greater than $\frac{\pi}{2}$, take $\frac{\pi}{2}$ as its value.

Step 3. **Update the circle pacing metric by DHGF.**

3.1. Compute edge lengths l_{ij} from the current vertices radius r_i and r_j and the fixed edge weight ϕ_{ij} using the cosine law (4).

3.2. Compute the corner angles θ_i in each face f_{ijk} from the current edge lengths by using the cosine law (3).

3.3. Compute the discrete Gaussian curvature K_i of each vertex v_i by using Eq.(2).

3.4. Update u_i of each vertex v_i by Eqs.(7).

3.5. Update r_i by Eqs.(5), and go to Step 3.1.

The following numerical experiments in this section show that this algorithm is not a very efficient algorithm for practical use due to the lowly convergence.

Examples

This numerical algorithm has been implemented in Java on a PC with AMD CPU of 3.4 GHz and 2GB RAM. We use Hypermesh to generat the triangle meshes for sphere, torus, and double torus(Fig.2).

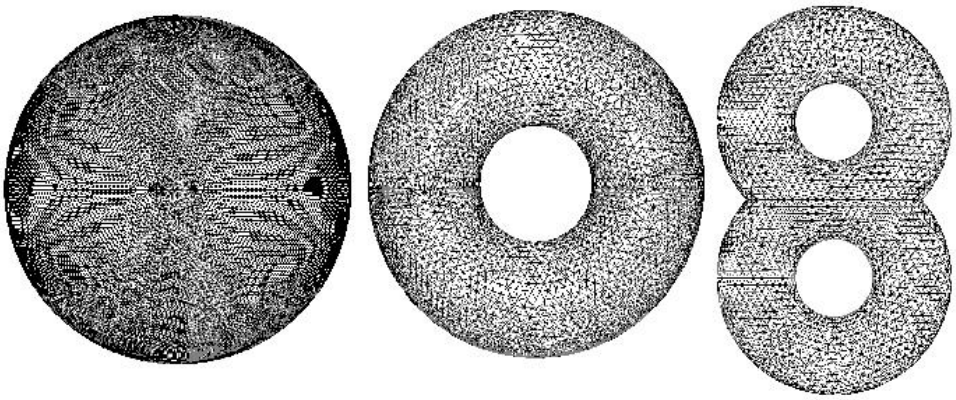

Figure 2: Triangle meshes for sphere, torus and double torus

For those meshes, we can calculate the initial value for $\{u_i^0, i \in V\}$ and let $u_i^0 = u_i^1$, for all $i \in V$, namely let the initial velocity be zero. Then we obtain a initial value problem for Eqs.(7) on sphere, torus and double torus.

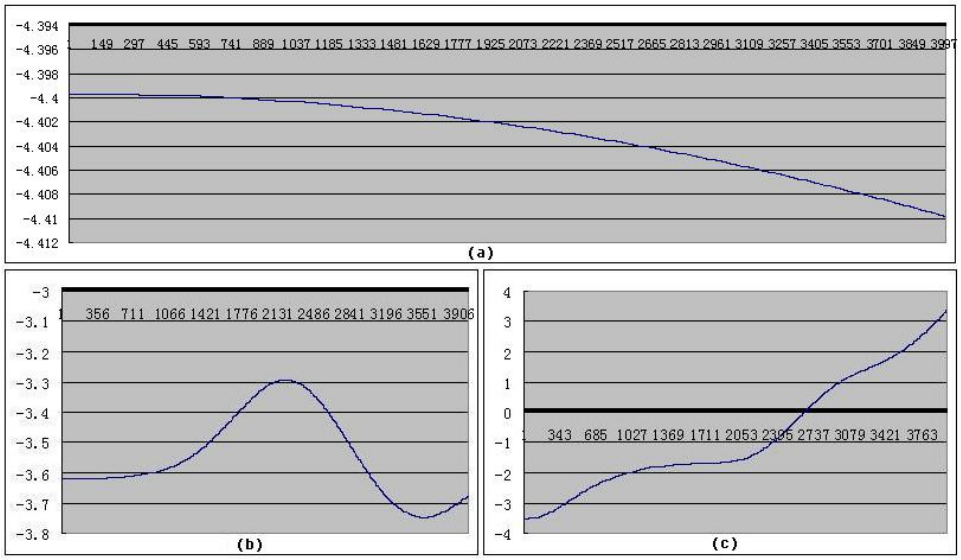

Figure 3: The trajectory of u_i under DHGF on different surfaces

Fig.3(a) shows the trajectory of one u_i in $\{u_i | i \in V\}$ on sphere for this initial value problems, (b) for torus, and (c) for double torus. Since the value of u_i on a vertex i can not give the information of others in $\{u_i | i \in V\}$, we let u be the mean value of $\{u_i | i \in V\}$ to describe the behavior of all u_i and record the initial and end values of u. Table 1 recodes the data of initial and end values of u for a initial value problem on sphere.

Δt	N	$u^0 = u^1$	u^N	r^N
0.0245	877	-4.399645598	-5.586009882	0.003778194
0.001	3999	-4.399645598	-4.409869389	0.012251197
0.0001	3999	-4.399645598	-4.399747835	0.012376393
0.00001	3999	-4.399645598	-4.3996466198	0.0123776606

Table 1 : Data for a initial value problem on sphere

The data in Table 1 and conclusion in Theorem 2.1(c) show that the discrete metric tend to 0 in infinite time. Since the Euler characteristic number of sphere

is 2 and the initial value satisfies $u^1 = u^0 < 0$, the trajectory of u is a parabola by Theorem 2.1(c). In Fig.4, it can be seen that the trend line for trajectory of u likes a parabola $y = ax^2 + b,\ a < 0,\ b < 0$. Fig.4(a) is the trajectory of u with $\Delta t = 0.024527068$, (b) with $\Delta t = 0.001$, (c) with $\Delta t = 0.0001$ and (d) with $\Delta t = 0.00001$.

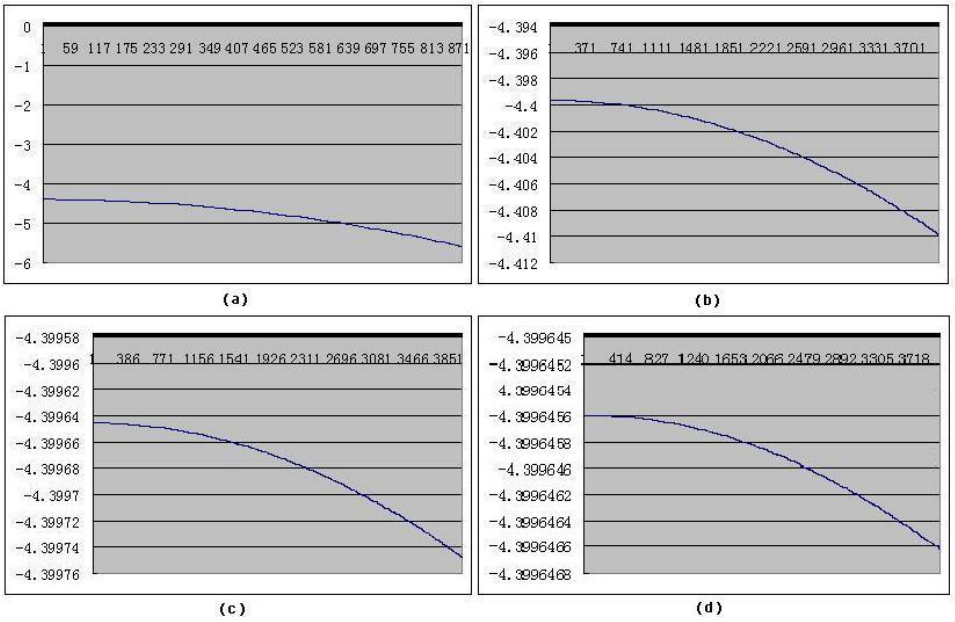

Figure 4: The trajectory of u under DHGF on sphere

Table 2 recodes the data of initial and end values of u for a initial value problem on double torus.

Δt	N	$u^0 = u^1$	u^N	r^N
0.01	3999	-3.074213079	3.404914496	32.27251434
0.001	3999	-3.074215499	-3.009424208	0.051216977
0.003	3999	-3.074215435	-2.491093808	0.124428483
0.0005	3999	-3.074215506	-3.058017683	0.047438238

Table 2 : Data for a initial value problem on double torus

Since the Euler characteristic number of double torus is -2 and the initial value satisfies $u^1 = u^0 < 0$, the trajectory of u is a parabola like $y = ax^2 + b,\ a >$

0, $b < 0$ by Theorem 2.1(a). In Fig.5, it can be seen that the trend line for trajectory of u is a parabola. Fig.5(a) is the trajectory of u with $\Delta t = 0.01$, (b) with $\Delta t = 0.001$, (c) with $\Delta t = 0.003$ and (d) with $\Delta t = 0.0005$.

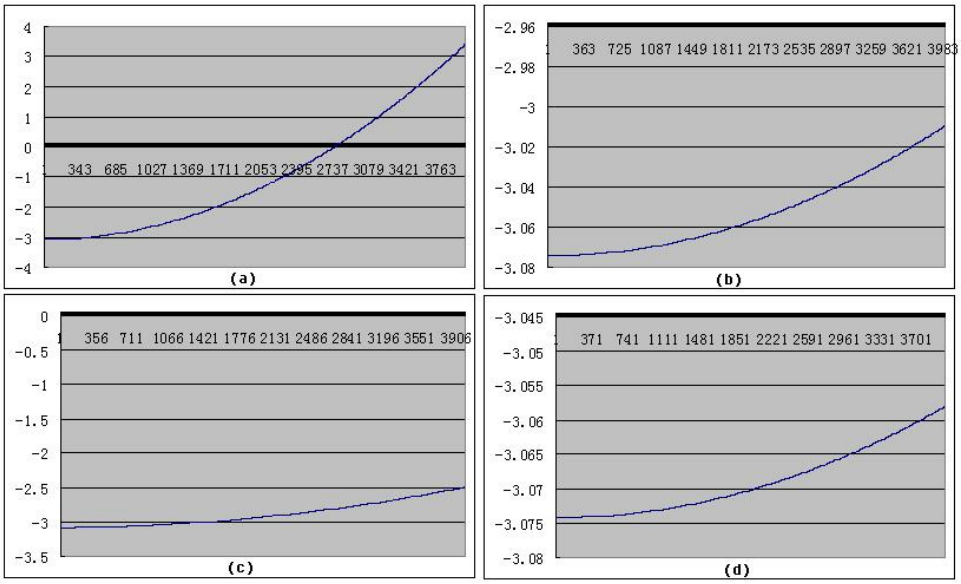

Figure 5: The trajectory of u under DHGF on double torus

Table 3 recodes the data of initial and end values of u for a initial value problem on torus.

Δt	N	$u^0 = u^1$	u^N	r^N
0.001	3999	-3.692617641	-3.692617641	0.025714392
0.0001	3999	-3.692617641	-3.692617641	0.025714392
0.0005	3999	-3.692617641	-3.692617641	0.025714392
0.00001	3999	-3.692617641	-3.692617641	0.025694951

Table 3 : Data for a initial value problem on torus

Since the Euler characteristic number of torus is 0 and the initial value satisfies $u^1 = u^0 < 0$, the trajectory of u is a straight line like $y = b,\ b < 0$ by Theorem 2.1(b). In Fig.6, it can be seen that the trend line for trajectory of u is a straight line. Fig.6(a) is the trajectory of u with $\Delta t = 0.001$, (b) with $\Delta t = 0.0001$, (c)

with $\Delta t = 0.0005$ and (d) with $\Delta t = 0.00001$.

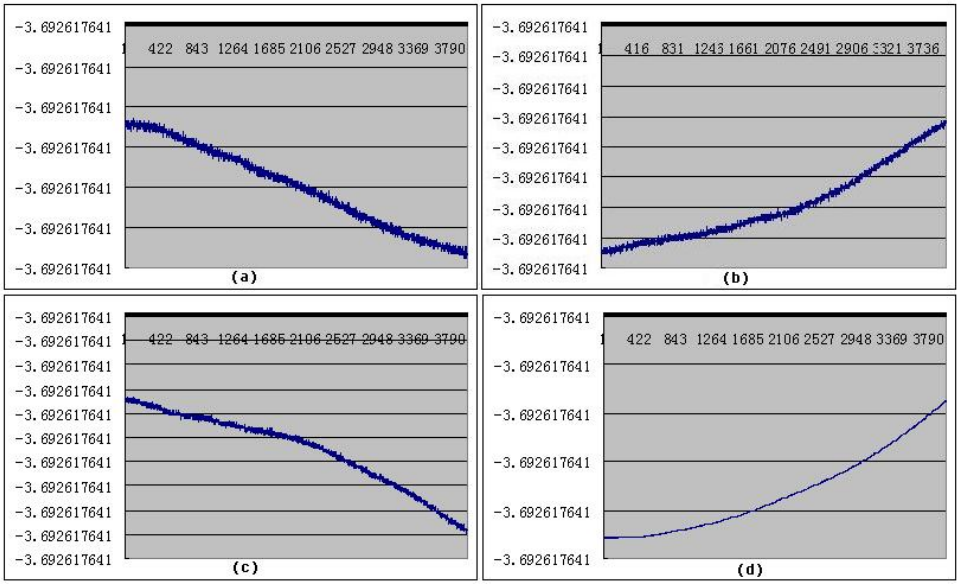

Figure 6: The trajectory for u of DHGF on torus

Based on data in Tables (1-3), we can obtain the qualitative behavior of mean value of discrete metric for three initial problems of DHGF (7) on different surfaces in Table 4.

Riemann sufaces	Euler characteristic	Initial discrete metric	Initial velocity	Mean value of metric
Sphere	2	< 1	0	Decay
Torus	0	< 1	0	Invariant
Double torus	-2	< 1	0	Expand

Table 4 : Summary of numerical results

3 Computation of HGF for pointwise conformal metric

Computational scheme

As the second part of our research, we are interested in calculating HGF on Riemann surfaces with pointwise conformal metric, namely the simplified HGF (2). The 2D space manifold can be approximated by triangles, and the time by line segments. We suppose each simplex contains its circumcenter and establish a discrete scheme for Eqs.(2) on triangles in Fig.7 as an example for a mesh, in which 0,..., C are vertices, 1, 2, 3 are the circumcenters of triangles, a, b, c are the circumcenters of edges. Letting l_{ij} be the length of line segment (i,j) and A_{ijkl} be the area of quadrangle (i,j,k,l), we approximate Eqs.(2) as follows:

$$\begin{aligned} w_O^{n+1} = 2w_O^n - w_O^{n-1} - \tfrac{2\Delta t^2}{P_O}\,(2\pi - \angle AOB - \angle AOC - \angle BOC) + \tfrac{\Delta t^2}{P_O}\Big(\tfrac{l_{13}}{l_{AO}} \\ \times(\ln w_A^n - \ln w_O^n) + \tfrac{l_{12}}{l_{BO}}(\ln w_B^n - \ln w_O^n) + \tfrac{l_{23}}{l_{CO}}(\ln w_C^n - \ln w_O^n)\Big). \end{aligned} \tag{9}$$

where $l_{12} := l_{1b} + l_{2b},\ l_{23} := l_{2c} + l_{3c},\ l_{31} := l_{3a} + l_{1a}$ and $P_O := A_{O1ab} + A_{O2bc} + A_{O3ac}$.

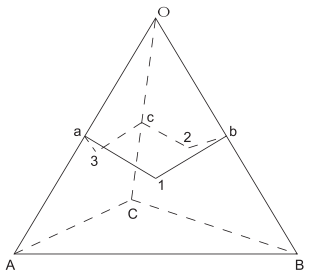

Figure 7: A part of triangle mesh

Analysis of stability

Suppose there is a perturbation ε_i^n on w_i^{n-1} and w_i^n on each vertice i, the relation between ε_i^n and ε_i^{n+1} can be induced from Eqs.(9) as follows:

$$\begin{aligned}\varepsilon_O^{n+1} &\approx \varepsilon_O^n + \frac{\Delta t^2}{P_O}\left(\frac{l_{13}}{l_{AO}}\left(\frac{\varepsilon_A^n}{w_A^n} - \frac{\varepsilon_O^n}{w_O^n}\right) + \frac{l_{12}}{l_{BO}}\left(\frac{\varepsilon_B^n}{w_B^n} - \frac{\varepsilon_O^n}{w_O^n}\right) + \frac{l_{23}}{l_{CO}}\left(\frac{\varepsilon_C^n}{w_C^n} - \frac{\varepsilon_O^n}{w_O^n}\right)\right)\\ &< \varepsilon_O^n - \frac{\Delta t^2}{P_O}\left(\frac{l_{13}}{l_{AO}} + \frac{l_{12}}{l_{BO}} + \frac{l_{23}}{l_{CO}}\right)\left(\frac{\varepsilon_O^n}{\max w_i^n} - \frac{\max \varepsilon_i^n}{\min w_i^n}\right)\\ &= \left(1 - \frac{\Delta t^2}{P_O}\left(\frac{l_{13}}{l_{AO}} + \frac{l_{12}}{l_{BO}} + \frac{l_{23}}{l_{CO}}\right)\frac{1}{\max w_i^n}\right)\varepsilon_O^n\\ &\quad + \frac{\Delta t^2}{P_O}\left(\frac{l_{13}}{l_{AO}} + \frac{l_{12}}{l_{BO}} + \frac{l_{23}}{l_{CO}}\right)\frac{\max \varepsilon_i^n}{\min w_i^n}.\end{aligned}$$

Therefore, we can say Eqs.(9) is unstable because

$$1 - \frac{\Delta t^2}{P_O}\left(\frac{l_{13}}{l_{AO}} + \frac{l_{12}}{l_{BO}} + \frac{l_{23}}{l_{CO}}\right)\left(\frac{1}{\max w_i^n} - \frac{1}{\min w_i^n}\right) > 1.$$

So we should choose very small time step to avoid numerical divergence rapidly. If the initial metric, initial velocity, and Gaussian curvature are isotropic, Eqs.(9) in this case is almost stable since $\max w_i^n \approx \min w_i^n$. The numerical experiment (Fig.8, Table.5) also verifies this point.

Geometric properties

The geometric property of Eqs.(9) shows that the Euler characteristic number has essential relationship with the solution. More specifically, we have

Theorem 3.1 *Let $\chi(\mathfrak{M})$ be the Euler characteristic number for closed Riemann surface $\mathfrak{M}$ with triangulation Σ. If $\{w_i^n | i \in V\}$ is a solution of Eqs.(9), then*

a. *If $\chi(\mathfrak{M}) > 0$, then any solution of Eqs.(9) decay in finite time for any initial value $\{w_i^0, w_i^1 | i \in V\}$.*

b. *If $\chi(\mathfrak{M}) = 0$ and $w_i^1 < w_i^0$ for all $i \in V$, then solutions of Eqs.(9) decay in finite time;*

c. *If $\chi(\mathfrak{M}) < 0$ and $w_i^1 \geq w_i^0$ for all $i \in V$, then solutions of Eqs.(9) expand in infinite time.*

Proof. Taking integration on both sides of Eqs.(9) and using Gauss-Bonnet formula, we have

$$\sum_{i\in V} w_i^n P_i = -2n(n-1)\pi\chi(\mathfrak{M})\Delta t^2 + n\sum_{i\in V} w_i^1 P_i - (n-1)\sum_{i\in V} w_i^0 P_i \qquad (10)$$

for $n \geqq 2$ and any initial conditions $\{w_i^1, w_i^0 | i \in V\}$. The conclusions (a-c) can be concluded from the expression (10). □

From the Theorem 3.1, we see that Eqs.(9) have essential geometric obstruction to the existence of periodic solution on sphere and double torus.

Examples

Table 5 records the value of one w_i in $\{w_i | i \in V\}$ on sphere for a special initial problems of Eqs.(9) with time step $\Delta t = 6.934 \times 10^{-6}$. Since the value of w_i can not give the information of others in $\{w_i | i \in V\}$, we let w be the mean value of $\{w_i | i \in V\}$ to describe the behavior of all w_i and record the value of w.

N	w_{i-1}^N	w_i^N	$\Delta \ln w_i^N$	k_i^N	w^N
1	1	1	0	1.53×10^{-7}	1
952	0.928424	0.928575	-1.23×10^{-8}	1.53×10^{-7}	0.931719
1903	0.708709	0.709017	1.60×10^{-9}	1.53×10^{-7}	0.72869
2854	0.356898	0.357318	7.72×10^{-8}	1.53×10^{-7}	0.392946
3488	0.0741055	0.0745791	1.07×10^{-8}	1.53×10^{-7}	0.0972911

Table 5 : Data for a initial value problem of Eqs.(9) on sphere

Since the Euler characteristic number of sphere is 2 and the initial value satisfies $w^1 = w^0 > 0$, the trajectory of $\sum_{i\in V} w_i^n P_i$ is a parabola like $y = ax^2 + b,\ a < 0,\ b > 0$ by Theorem 3.1(a). So w is almost a parabola if $P_i \approx P_j,\ \forall\ i, j \in V$. Fig.8(a) is the trajectory of one w_i and (b) is a trajectory of w. It can be seen

that the trend line in Fig.8(b) is a parabola.

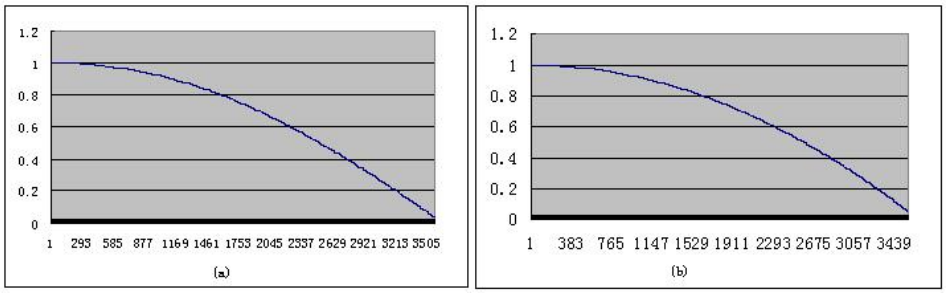

Figure 8: The trajectory of a w_i and w of Eqs.(9) on sphere

Table 6 shows the data for a special initial problems for Eqs.(9) on torus with time step $\Delta t = 2.8311 \times 10^{-5}$.

N	w_{i-1}^N	w_i^N	$\Delta \ln w_i^N$	k_i^N	w^N
1	1	1	0	7.83×10^{-8}	1
1255	0.929713	0.929832	-1.58×10^{-8}	7.83×10^{-8}	0.957312
2509	0.437896	0.438117	7.53×10^{-7}	7.83×10^{-8}	1.00795
3345	0.432457	0.432378	7.95×10^{-7}	7.83×10^{-8}	1.02469
4366	0.438288	0.438177	1.02×10^{-6}	7.83×10^{-8}	0.910947

Table 6 : Data for a initial value problem of Eqs.(9) on torus

Since the Euler characteristic number of torus is 0 and the initial value satisfies $w^1 = w^0 > 0$, the trajectory of $\sum_{i \in V} w_i^n P_i$ is a line like $y = b,\ b > 0$ by Theorem 3.1(b). So w is almost a line if $P_i \approx P_j,\ \forall\ i, j \in V$. Fig.9(a) is the trajectory of one w_i in $\{w_i | i \in V\}$ and (b) is a trajectory of w. It can be seen that the trend line for trajectory of w is almost a line. The trajectory in Fig.9 (b) is not exact a line, in part because the anisotropy of the curvature and the irregularity of mesh. The value of w will neither decay nor expand. If $w_i^{+\infty} = +\infty$, then $\sum_{i \in V} w_i^{+\infty} P_i = +\infty$, which contradicts to Theorem 3.1(b). If there is a N such that $w_i^N = 0$ and $w_j^N \neq 0$ for a pair of adjacent points i, j, then $\Delta \ln w_j^N = \infty$, so

$w_j^{N+1} = \infty$, which contradicts with Theorem 3.1(b). So w will always oscillate.

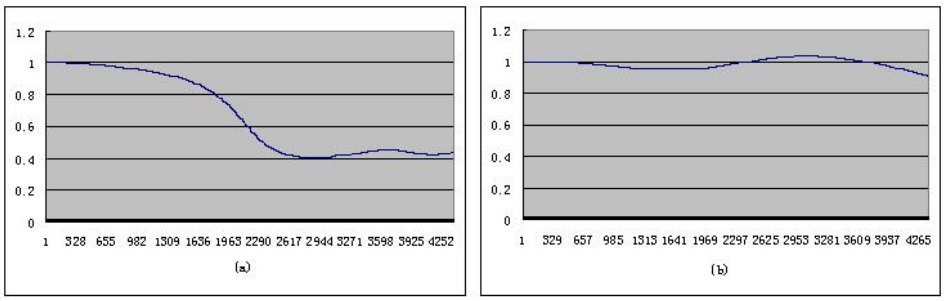

Figure 9: The trajectory of a w_i and w of Eqs.(9) on torus

Table 7 records the data for a special initial problems for Eqs.(9) on double torus with time step $\Delta t = 2.8311 \times 10^{-5}$.

N	w_{i-1}^N	w_i^N	$\Delta \ln w_i^N$	k_i^N	w^N
1	1	1	0	1.48×10^{-8}	1
4000	0.922261	0.922296	3.48×10^{-9}	1.48×10^{-8}	1.03876
8000	0.724934	0.724994	8.16×10^{-9}	1.48×10^{-8}	1.15113
12000	0.487802	0.48785	3.75×10^{-8}	1.48×10^{-8}	1.34347
14629	0.451264	0.45125	3.23×10^{-8}	1.48×10^{-8}	1.51792

Table 7 : Data for a initial value problem of Eqs.(9) on torus

Since the Euler characteristic number of double torus is -2 and the initial value satisfies $w^1 = w^0 > 0$, the trajectory of $\sum_{i \in V} w_i^n P_i$ is a parabola like $y = ax^2 + b$, $a > 0, b > 0$ by Theorem 3.1(c). So w is almost a parabola if $P_i \approx P_j$, $\forall\ i, j \in V$. Fig.10(a) is the trajectory of one w_i and (b) is a trajectory of w. It

can be seen that the trend line for trajectory of w is almost a parabola.

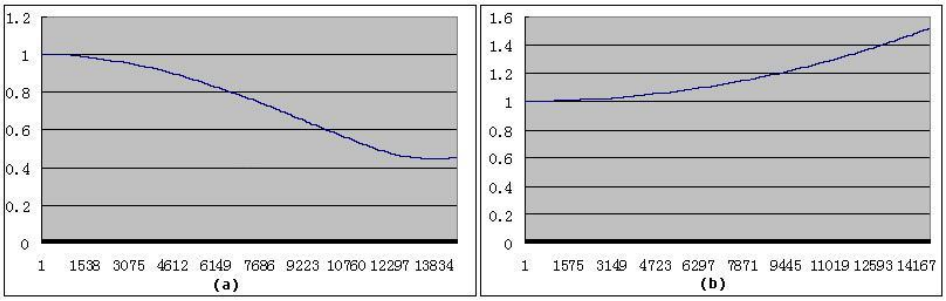

Figure 10: The trajectory of a w_i and w of Eqs.(9) on double torus

Based on data in Tables (5-7), we can obtain the qualitative behavior of mean value of discrete metric for three initial problems for Eqs.(9) on different surfaces in Table 8. It can be see that our numerical results verify the conclusion of Kong and Liu et al: if the Euler characteristic number of surface is positive, then any solution of Eq.(2) must blow up in finite time for any initial problem [11].

Riemann sufaces	Euler characteristic	Initial discrete metric	Initial velocity	Mean value of metric
Sphere	2	> 0	0	Decay
Torus	0	> 0	0	Oscillation
Double torus	-2	> 0	0	Expand

Table 8 : Summary of numerical results

4 Conclusion

We have introduced two algorithms for HGF with circle packing metric and pointwise conformal metric respectively that allow to study HGF in computing view. The experimental results are consistent with the theoretical achievement by Kong and Liu. This proofs the correctness and effectiveness of those algorithms at a certain extent. One limitation of the method for the experiments that we performed was the dependence of the high qualitative triangulation for Riemann surfaces, namely, each triangle should be acute one. The other limitation is the computation time. It is interesting to note that the speed of our algorithms

can be substantially improved by using some method, for instance by Newtonian iteration.

5 Future work

Boundary conditions

The discrete Gaussian curvature can also be defined as the angle deficit on a boundary of meshes as

$$K_i = \pi - \sum_{f_{ijk} \in F} \theta_i^{jk}$$

where θ_i^{jk} represents the corner angle attached to vertex v_i in the face f_{ijk}. Hence, we can consider the mixed initial boundary value problem for hyperbolic geometric flow.

Open regions

A consideration with numerical approach to solving HGF is that many geometries of interest are defined in open regions where the spatial domain of the computed field is unbounded in one or more coordinate directions, e.g., $\mathbb{R}^2$. Principally, this is because those scheme in this paper cannot be implemented at the outermost vertices, since by definition there is no information concerning the curvature value outside of computational domain.

Singularities

It well known that one can understand the heat kernel from the kernel of wave equation. This indicates that one can derive various information of the Ricci flow from that of the HGF. Therefore it is also interesting to understand the relations between the HGF and the Ricci flow, the singularities of its solutions and its relation by numerical method. This will be another interesting topic to exploration.

Acknowledgements The author Z. Xie would like to express his deep gratitude to Professors K.F. Liu and D.X. Kong in Zhejiang University for several constructive suggestions and the useful information concerning the content of this paper.

References

[1] R.S. Hamilton, The Ricci flow on surfaces, Mathematics and general relativity, vol. 71, 237-262, (1988).

[2] R.S. Hamilton, Three-manifolds with positive Ricci curvature, J. Differential Geom. 17, 255-306, (1982).

[3] V. Fock, The theory of space, time and gravitation, second revised edition. Translated from the Russian by N. Kemmer. A Pergamon Press Book The Macmillan Co., New York, 1964.

[4] R. Penrose, Gravitational collapse and space-time singularities, Phys. Rev. Lett. 14, 57-59, (1965).

[5] H.D. Cao, X.P. Zhu, A complete proof of the Poincaré and geometrization conjectures application of the Hamilton-Perelman theory of the Ricci flow, Asian J. Math. 10, 165-492, (2006).

[6] W.-R. Dai, D.-X. Kong & K.-F. Liu, Dissipative hyperbolic geometric flow, *Asian J. Math.* 12 (2008), 345-364.

[7] D.-X. Kong, Hyperbolic geometric flow, *the Proceedings of ICCM 2007*, Vol. II, Higher Educationial Press, Beijing, 2007, 95-110.

[8] D.-X. Kong & K.-F. Liu, Wave character of metrics and hyperbolic geometric flow, *J. Math. Phys.* 48 (2007), 103508.

[9] D.-X. Kong, K.-F. Liu & Y.-Z. Wang, Life-span of classical solutions to hyperbolic geometric flow in two space variables with slow decay initial data, to appear in *Communications in Partial Differential Equations*.

[10] D.-X. Kong, K.-F. Liu & D.-L. Xu, The hyperbolic geometric flow on Riemann surfaces, *Communications in Partial Differential Equations* 34 (2009), 553-580.

[11] K.D. Xing; K.F. Liu, Wave character of metrics and hyperbolic geometric flow, Journal of Mathematical Physics, Volume 48, Issue 10, (2007).

[12] W.-R. Dai, D.-X. Kong & K.-F. Liu, Hyperbolic geometric flow (I): short-time existence and nonlinear stability, *Pure and Applied Mathematics Quarterly (Special Issue: In honor of Michael Atiyah and Isadore Singer)* 6 (2010), 331-359.

[13] A.E. Fischer and J.E. Marsden, The Einstein evolution equations as a first order quasi linear symmetric system hyperbolic system I, Commun. Math. Phys. 28, 1-38, (1972).

[14] Fu Wen Shu and You Gen Shen, Geometric flows and black holes, arXiv: gr-qc/0610030.

[15] B. Chow, F. Luo, Combinatorial Ricci flows on surfaces, J.differential geometry, 63, , 97-129, (2003).

[16] W.P. Thurston, Geometry and Topology of Three-Manifolds. Princeton lecture notes, (1976).

[17] F. Luo, Variational Principles on Triangulated Surfaces. http://arxiv.org/abs/0803.4232v1.

[18] M. Jin, J. Kim, F. Luo, X.F. Gu, Discrete surface Ricci flow, IEEE Transactions on Visualization and Computer Graphics, Volume 14, Issue 5, (2008).

[19] W.-R. Dai, D.-X. Kong & K.-F. Liu, Hyperbolic geometric flow (I): short-time existence and nonlinear stability, *Pure and Applied Mathematics Quarterly (Special Issue: In honor of Michael Atiyah and Isadore Singer)* 6 (2010), 331-359.

Zheng Xie
Department of Systems Engineering and Mathematics,

National University of Defense Technology,
Changsha, (410073), China
E-mail: lenozhengxie@yahoo.com.cn

Zheng Ye
College of Computer Science & Information Engineering,
Zhejiang Gongshang University,
Hangzhou, (310018), China